Low-frequency Raman study of the ferroelectric phase transition in a layered CuCl$_4$-based organic-inorganic hybrid

Antonio Caretta, Rany Miranti, Remco W. A. Havenith, Elia Rampi, Michiel C. Donker, Graeme R. Blake, Matteo Montagnese, Alexey O. Polyakov, Ria Broer, Thomas T. M. Palstra, and Paul H. M. van Loosdrecht[*]

Zernike Institute for Advanced Materials, University of Groningen, Nijenborgh 4, 9747 AG Groningen, The Netherlands
(Received 12 September 2012; revised manuscript received 17 September 2013; published 6 January 2014)

The ferroelectric phase transition at $T_C = 340$ K in $(C_6H_5CH_2CH_2NH_3)_2CuCl_4$ is studied by means of temperature-dependent low-frequency Raman scattering, focusing on the coupling of a low-energy librational mode to the order parameter of the transition. Analysis of the symmetry and characteristics of this mode links the dipolar order to the tilt angle of the organic cations. The thermal evolution of the Raman spectrum demonstrates the displacive component of the phase transition in combination with order-disorder phenomena and the importance of the organic-inorganic interplay to the physical properties of the compound. The ferroelectric properties investigated here can be generalized to the family of layered organic-inorganic hybrids.

I. INTRODUCTION

Inorganic materials exhibit a rich variety of electronic properties and phenomena, including ferroelectricity, ordered magnetism, spin liquid behavior, (high-temperature) super-conductivity, and Mott metal-insulator transitions. Although their properties can be tuned to a limited extent by chemical doping and/or substitution, they are not as versatile as organic materials. Additionally, organic materials usually have the advantage of relatively cheap and easy processability, for instance, through spin coating. In this respect, organic-inorganic hybrid (OIH) materials—the crystalline combination of typical inorganic structures with organic molecules—form an interesting class of materials combining the best of both worlds' properties.

A general and useful approach to classify these hybrids is to consider the dimensionality of the connectivity of the constituents.[1] The best-known OIHs are probably the coordination polymers and/or metal organic frameworks,[2] which, with their high degree of organic connectivity, form a large subclass of OIHs. They are widely studied, particularly in view of their potential applications in catalysis, gas separation, and storage.[3,4]

In this paper, we focus on hybrids with two-dimensional *in*organic connectivity in which the inorganic part has a structure reminiscent of the perovskites.[5] The well-connected inorganic constituents provide robust interactions leading to functional electronic, magnetic, and optical properties.

This family of OIHs has, in particular, been widely studied for its intriguing magnetic properties[6] and structural phase transitions.[7,8] The perovskite-based crystals have the general formula A_2MX_y or $A'MX_y$, where M is a transition metal, X's are typically halogen atoms (with $y = 3,4$), and A (A')'s are monovalent (divalent) organic cations. These materials are the ideal systems for studying the physics of low-dimensional magnetism[6] because the distance between inorganic constituents can be tuned by varying the organic molecules. In particular, one-dimensional- ($y = 3$) (Refs. 9 and 10) and two-dimensional-[11,12] ($y = 4$) type hybrids offer the opportunity to investigate the implications of the Mermin-Wagner theorem.[13] One surprising finding is that the layered CuCl$_4$-based crystals undergo ferromagnetic ordering with critical temperatures

exceeding 10 K.[14,15] A second focus in the research on layered OIHs concerns the structural phase transitions that often are found at high temperatures. These layered hybrids have a simple structure:[5] corner-sharing metal halide octahedra form isolated chessboardlike layers; the organic molecules fill the space between the layers of octahedra, attached on both sides of a given layer by hydrogen bonding via an ammonium head group. As observed by Petzelt,[16] two types of orthorhombic structures are typically adopted at room temperature: a more symmetric one ($Cmca$, D_{2h}^{18}), generally found for manganese compounds, and a more distorted one ($Pbca$, D_{2h}^{15}), typical for copper compounds. The difference between these two structures is due to the Jahn-Teller activity of the Cu^{2+} ions. Interest in these layered-type hybrids has been triggered by the frequent observation of a complex cascade of phase transitions that often occur well above the magnetic ordering temperature. The variety of structural and physical phenomena found in this family of compounds can be ascribed to the large differences in interaction strengths and length scales associated with the chemical bonding: The organic molecules and inorganic layers are composed of strong covalent and ionic bonds, respectively; both ionic and hydrogen bondings are of importance at the organic-inorganic interface, and van der Waals forces largely govern the molecular arrangement in the organic layers. A large number of experiments have been performed in order to reveal the origin of the various physical phenomena in layered hybrids: x-ray diffraction,[17–19] differential scanning calorimetry,[17,20] birefringence and microscopy,[17–22] NMR and ^{35}Cl nuclear quadrupole resonance[23–26] (NQR), Brillouin scattering,[27] neutron diffraction,[28,29] ultrasound experiments,[30,31] and IR/Raman spectroscopy (e.g., Refs. 32–35). The most widely accepted picture is that the high-temperature phase transitions are caused by reorientational order-disorder dynamics of the organic cation, more specifically, that of the NH$_3$ head group as already discussed in early group-theory studies[16] and NQR work.[23] Although experiments are generally in good agreement with this model, a number of studies have indicated that the inorganic moiety also plays a role in the phase transitions.[34,36] Soft-mode condensation models have also been described for similar compounds,[16,37–39] but experimental studies of soft-mode behavior[30,32] have not

yet clearly demonstrated a high-temperature transition with displacive characteristics in the layered hybrids.

Interest in the layered $CuCl_4$-based hybrids has recently been renewed by the observation of combined ferromagnetic and polar orders.[40,41] We note that both ferroelectric and antiferroelectric orderings had previously been reported in perovskite-based OIHs with one-dimensional inorganic connectivity.[42,43] However, the structural phase transitions observed in the layered-type hybrids, although widely investigated, had never been connected to polar ordering until recently when the possibility of combined ferromagnetic and ferroelectric order and, consequently, multiferroicity was considered.[44–46] A prime example of a perovskite-based layered hybrid undergoing both ferromagnetic ($T = 13$ K) and ferroelectric ($T = 340$ K) ordering is $(C_6H_5CH_2CH_2NH_3)_2CuCl_4$ (Ref. [40]) (PEACuCl), the subject of this paper.

The physical origin of the ferroelectric phase transition at 340 K in PEACuCl is still under debate. The models of dipolar ordering that have, thus far, been used for layered CuCl hybrids[40,41] are based on the previously mentioned reorientational disorder dynamics of the NH_3 group in the rigid multifold potential of the inorganic layers. However, our analysis suggests that the phase transition at 340 K in PEACuCl also has a displacive character, involving tilting of the polar organic molecules. In particular, this paper shows that interplay between the organic and the inorganic moieties, which has previously often been neglected, plays a fundamental role in determining the physical properties of the compound. Furthermore, the presence of similar phase transitions in most of the layered hybrids suggests that the results obtained here for PEACuCl can be generalized to other compounds in the same family. The general aspects of displacive phase transitions have been investigated over the past 50 years, focusing on concepts, such as stability and ferroelectricity,[47] soft modes and symmetry,[48–50] and dielectric response and mode softening.[51,52] The results presented in these papers are fundamental to the discussion of the origin of the ferroelectric ordering observed in layered CuCl-type hybrids.

In order to investigate the origin of the onset of polar order in PEACuCl at 340 K, we performed temperature-dependent polarized low-frequency Raman scattering, terahertz (THz) absorption experiments, and density functional theory (DFT) calculations. Low-frequency Raman/IR modes are often directly coupled to the order parameter of a phase transition[53,54] and, thus, provide information about the dipolar order. As we will discuss below, the temperature dependence of some of the phonons, indeed, provides clear evidence of a connection between the structural symmetry modification and the appearance of a polar state below 340 K. Before addressing this issue, however, we will first discuss the experimental approach, the DFT results, and will summarize the general features of the low-frequency polarized Raman/IR spectra of PEACuCl, which are typical of many of the layered OIHs.

II. EXPERIMENTAL DETAILS

The hybrid compound PEACuCl is a layered ferromagnetic and pyroelectric insulator.[40] Transparent square platelet crystals were obtained by slow evaporation from solution.[55] The platelets are c oriented with edges typically along $a' = (a + b)$ and $b' = (a - b)$, where a and b are the orthorhombic axes in the plane.

At room temperature, the thermochromic crystals are yellowish but turn green on cooling below $\sim$200 K.[21,56,57] The crystal structure has previously been determined by x-ray diffraction.[58] The inorganic $CuCl_6$ octahedra share corners to form two-dimensional sheets separated by a bilayer of organic molecules, here phenylethylammonium (PEA).[5,59] At 100 K, x-ray-diffraction data suggested that the nonpolar $Pbca$ space group (D_{2h}^{15}) is adopted. However, pyroelectric current measurements have shown that PEACuCl is polar below 340 K, hence, the actual space group must be polar.[40,60] The true space group is not yet known, and we will, thus, use the Porto notation to indicate the symmetry of the vibrational modes. The unit cell ($7.21 \times 7.27 \times 38.24$) Å^3 is composed of 188 atoms, corresponding to 4 formula units per unit cell [for a schematic of the unit cell, see the inset of Fig. 2(b) or Refs. 5 and 60]. At 13 K, the material undergoes a magnetic transition to a ferromagnetically ordered state where the easy axis lies in the inorganic plane.[15,40] The ferroelectric polarization is not the primary order parameter of the transition[48] but only a function of it, thus, the ferroelectric ordering at $\sim$340 K has an improper character. This can be evinced, for instance, by the non-Curie-Weiss behavior of the dielectric function[52,61,62] above T_C.[40]

Polarized Raman spectroscopy measurements were performed in backscattering configuration using a triple grating micro-Raman spectrometer (T64000, Jobin Yvon). The resolution of the spectrometer is better than 2 cm^{-1}. The sample was mounted on the cold finger of an optical flow cryostat with a temperature stabilization better than 0.1 K. The 647-nm laser line of a krypton laser was used to excite the sample, keeping the fluence on the sample below 5 kW cm^{-2}. Throughout this paper, we will use the Porto notation (x,y) to indicate the polarization of the incoming (x) and scattered (y) light.

THz measurements were performed using a THz transmission spectrometer, which has previously been described.[63] The propagation direction was parallel to the c axis of the sample, and the electric-field polarization of the THz pulse was in the ab plane.

Vibrational frequencies and eigenmodes at the Γ point of the low-temperature phase were calculated with periodic unrestricted DFT [following Ref. 64 with the Perdew-Burke-Ernzerhof (PBE) functional] using the CRYSTAL (Refs. 65–68) package with the Doll basis set for Cu,[69] the Aprà basis set for Cl,[70] and the 6-21G* basis set for C/N/H (Refs. 71–73) (CRYSTAL basis set web page[74]). The crystal was optimized with (ion positions) and without (both ion positions and cell parameters) symmetry constraints at $T = 0$ K (in the ferromagnetic state). The k points were selected according to the procedure of Monkhorst-Pack[75] for a $4 \times 4 \times 4$ mesh.

III. DFT CALCULATIONS

The DFT calculations suggested that the real symmetry of the structure might be lower than the experimentally suggested $Pbca$ structure in agreement with the observed pyroelectric behavior.[40] The first optimization was performed

TABLE I. Experimental structural parameters of PEACuCl determined in space group $Pbca$ at 100 K (labeled 100 K) compared with parameters obtained from the $T = 0$-K DFT calculations with and without symmetry constraints (labeled $Pbca$ and "$P1$," respectively). We note that, both for the in-plane Cu-Cl distances (CuCl-1 and CuCl-2) and for the out-of-plane distance (CuCl-3), two different values are allowed for $P1$ symmetry.

Structure	a (Å)	b (Å)	c (Å)	α (°)	β (°)	γ (°)	CuCl-1 (Å)	CuCl-2 (Å)	CuCl-3 (Å)	θ_B (°)
100 K	7.21	7.27	38.24	90	90	90	2.288	2.853	2.304	6.6
$Pbca$	7.21	7.27	38.24	90	90	90	2.374	2.780	2.432	6.5
$P1$	7.57	7.41	36.82	89.8	92.2	89.9	2.366–2.341	2.983–3.021	2.472–2.475	18.1

within the experimentally derived unit cell (at 100 K, $a = 7.21$, $b = 7.27$, and $c = 38.24$ Å) and space group ($Pbca$) as an approximation. The resulting Cu-Cl distances and the buckling angle θ_B of the inorganic octahedra are in good agreement with the experimental values (see Table I). The structural parameters associated with the organic groups are in line with the experimental values. However, the frequency calculation showed that this structure does not correspond to a genuine minimum. Four imaginary frequencies of 36 cm^{-1} (B_{2u}), 33 cm^{-1} (B_{1g}), 22 cm^{-1} (A_g), and 20 cm^{-1} (A_u) were found. Symmetry reduction along these imaginary modes results in a structure with $P1$ symmetry. Accordingly, the crystal structure was fully optimized (including the unit-cell parameters) in $P1$. The optimized structure has lattice parameters of $a = 7.57$, $b = 7.41$, $c = 36.82$ Å, $\alpha = 89.8°$, $\beta = 92.2°$, and $\gamma = 89.9°$, which are within 5% of the experimentally determined lattice parameters. The Cu-Cl distances deviate somewhat from the experimentally derived parameters in $Pbca$ but are still within 5%. A summary of the relevant structural parameters is given in Table I. It should be noted that the deviation in the buckling angle from the experimental value ($\theta_B = 6.6°$) is considerably larger: $\theta_B = 18.1°$. For this structure, no imaginary frequencies were found. A very rough estimate of the possible electric dipole per unit cell was obtained by calculating the dipole moment from the Mulliken charges: This leads to a dipole moment of

41 D (1 D $= 3.34 \times 10^{30}$ C m). The direction of this dipole is in the ab plane, and it makes an angle of 29° with respect to the b axis. We note that this is only indicative for the possibility of a dipole moment that lies within the ab plane.

We now focus our attention on the calculated vibrational modes and, in particular, on the modes below 60 cm^{-1} since, as will be shown later, these carry the most important information on the structural phase transition in the high-temperature range. A comparison of the calculations involving the most intense modes below 400 cm^{-1} is given in Table III; comparing the calculated frequencies and the measured high-energy modes is difficult because of the large number of vibrations above 400 cm^{-1} (approximately 400 modes), but the agreement was, in general, good. The modes between 10 and 30 cm^{-1} can be represented as three types of shear mode of the organic layers with respect to the inorganic layers. As depicted in Table II, the lowest-energy mode, type 1 in the table, can be represented as a bending of the unit cell along the central inorganic layer. We note that there are two nearly degenerate modes per shear type; the modes can be distinguished by the displacement direction in the ab plane (shown in the second column of the table). The type-2 modes at ~ 20 cm^{-1} involve out-of-phase shear of the two organic moiety bilayers. The type-3 shear modes at ~ 25 cm^{-1} can be described as in-phase shear of the organic layers in contrast to the type-2 modes. For the type-3 modes, the intrinsic dipole

TABLE II. (Color online) DFT-calculated displacement scheme of the low-frequency Raman/IR modes in PEACuCl. The red lines and red arrows represent the distortion of the unit cell with respect to the equilibrium position drawn in black. In the table are depicted (from left to right): (i) the side view of the unit cell perpendicular to the b axis, (ii) the top view perpendicular to the c axis (there are two nearly degenerate modes per shear mode), (iii) the calculated frequency according to $Pbca$ symmetry, and (iv) to $P1$ symmetry. The intrinsic dipole of the PEA molecule also is drawn with a green arrow for the type-3 mode displacements.

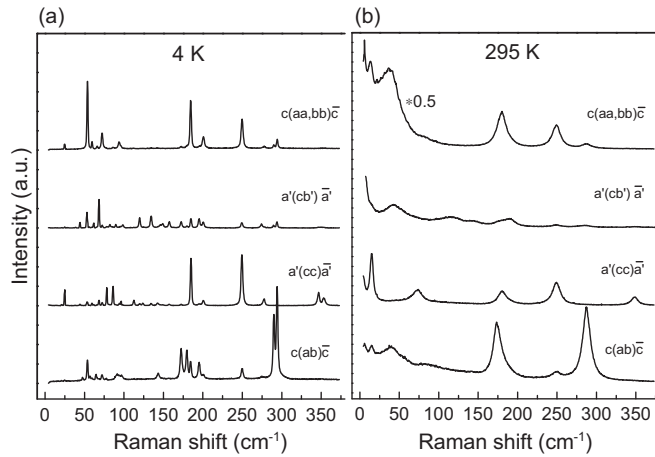|	Displacements scheme		Frequency (cm^{-1})	
No.	Side view	Top view	$Pbca$	$P1$
(1)			11.1 (B_{1u}) -20 (A_u)	11.2 11.7
(2)			-22 (A_g) 23.2 (B_{1g})	16.6 21.6
(3)			23.1 (B_{3u}) 33.7 (B_{2u})	23.8 26.9

FIG. 1. Overview of low-energy phonons at (a) 4 K and (b) 295 K with their symmetry configurations. The energy assignment of the modes is given by comparison with similar $CuCl_4$-based hybrids (see Table III). Note that Porto notation is used with $a' = (a + b)$ and $b' = (a − b)$.

of the organic molecules is indicated by arrows. Later, we will show that these modes are very interesting because they represent the only low-energy vibration that can lead to dipolar ordering. Finally, the modes between 30 and 60 cm^{-1} can be represented by various c-axis rotational modes of both the PEA cations and the inorganic octahedra, although a modest mixture of shear and squeezing motion is always present. It is interesting to note that the DFT calculation shows that most modes below 200 cm^{-1} have a strong organic-inorganic librational character.

IV. VIBRATIONAL PROPERTIES

Group-theory analysis predicts that, for $Pbca$ (D_{2h}^{15}) symmetry, there are 276 Raman active modes and 216 IR modes. Above 400 cm^{-1}, the Raman active modes are pure stretching modes of the organic cation.[76,77] The mode assignment and thermal evolution of the high-energy intramolecular organic vibrations studied for similar compounds [e.g., $(C_nH_{2n+1}NH_3)_2CuCl_4$] have previously given evidence for the rotational disorder of the NH_3 group.[76–78] The Raman active CuCl modes, low-energy bending modes of the cation,

and external lattice modes are found in the spectral region below 400 cm^{-1}.[33] The polarized Raman spectra of PEACuCl in this region are shown in Fig. 1 where the left panel (a) displays the 4-K spectra and the right panel (b) displays the room-temperature spectra. Table III summarizes the most intense observed modes at $T = 4$ and 296 K, together with the measured configuration and assignments based on DFT predictions. For simplicity, hereafter, we will refer to the phonons by their room-temperature Raman shifts. The assignment of the modes above $\sim 60\ cm^{-1}$ was performed by comparison with previous reports on similar materials. The modes at 172, 180, 249, and 287 cm^{-1} are pure octahedral vibrations[33,35] of the inorganic constituents. The mode at 348 cm^{-1} is composed of a skeletal CCCN bending and a NH_3 torsion.[77,79] The mode at 73 cm^{-1} had previously been assigned to a $CuCl_6$ libration mode.[80] However, from a comparison with the Raman spectra of related compounds, we conclude that it is actually a translational mode of the cations perpendicular to the layers. For compounds with a lighter cation, this mode is found at 130 cm^{-1} [methylammonium (MA)] and [ethylammonium (EA)].[32] For PEACuCl, one finds, from a simple mass scaling of the frequency (i.e., assuming that the interaction strengths are similar), a value of 66 cm^{-1}, which is very close to the observed frequency. The DFT calculations are in good agreement with this mode assignment. The only discrepancy concerns the $c(ab)\bar{c}$ mode at 287 cm^{-1}, which previously was described as a CuCl mode in a study of MACuCl.[35] Such a mode should also appear for PEACuCl, but the DFT calculation assigns it as a cationic bending (with four nodes along the long axis).

The Raman/IR active modes below 60 cm^{-1} have a librational organic-inorganic origin and probe the most interesting aspects of the 340-K phase transition. A displacive phase transition is, in general, partnered by the softening of collective excitations[47,82,83] (soft modes), which are observable in the Raman and/or IR spectra.[49,50] Indeed, two modes show a distinct temperature dependence, which at room temperature, are observed at 15 and 40 cm^{-1} (from here on referred to as α and β, respectively). Mode α is both Raman active—possibly totally symmetric, being active in parallel configuration—and IR active in the distorted phase. Approaching T_C from below, the mode intensity, as we will show later, couples to the order parameter of the phase transition and disappears in the high-temperature phase. Such behavior is consistent with

TABLE III. Raman active modes below 400 cm^{-1} observed at room temperature (frequencies at $T = 4$ K are given in parentheses), together with their symmetry. Note that the symmetry notation (xy) refers to the (xy) probed element of the Raman tensor [e.g., (ab) corresponds to $c(ab)\bar{c}$, and (aa) corresponds to $c(aa)\bar{c}$].

| Mode frequencies (cm^{-1}) at $T = 296$ K (4 K)	Symmetry	Assignment	DFT calculations ($T = 0$ K)
15 (25): α	(aa,bb,cc)	Librational[32]	Table II
40 (53): β	(aa,bb)	Librational[32]	PEA z rotations
73 (76 + 86)	(cc)	PEA z translational[32,80,81]	PEA z translational and rotational
172 (174)	(ab)	CuCl (Ref. 33)	CuCl in-phase in plane
180 (184)	(aa,bb,cc)	CuCl (Ref. 35)	CuCl out-of-phase in plane
248 (249)	(aa,bb,cc)	CuCl (Ref. 35)	CuCl full in phase
287 (288 + 295)	(ab)	CuCl (Ref. 35)	PEA bending
348 (346 + 353)	(cc)	NH_3, CCCN (Refs. 77 and 79)	NH_3 librations
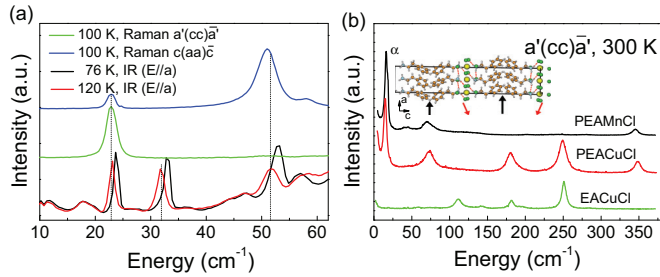
FIG. 2. (Color online) (a) IR and Raman spectra in the low-frequency range around 100 K. The α mode is both Raman and IR active. (b) Comparison of the room temperature $a'(cc)\overline{a'}$ Raman spectra of PEACuCl (middle curve), PEAMnCl (top curve), and EACuCl (lower curve). The inset shows a schematic of the displacements associated with the Raman/IR mode α, which is found at 15 cm^{-1} (at 300 K) for both PEA compounds as obtained from DFT calculations (red and black arrows, respectively, indicate the inorganic and organic displacement directions; see also Table II).

FIG. 3. (Color online) Temperature evolution of low-energy phonons α, at ~15 cm^{-1} (a) $a'(cc)\overline{a'}$ and β at ~40 cm^{-1} (b) $c(aa)\overline{c}$. On heating, the modes continuously soften and broaden. The intensity of α decreases to zero at T_C, indicating a change in symmetry in the system. In contrast, β is still Raman active above T_C. The measured intensity I_{meas} is scaled as $I_{\mathrm{red}} = I_{\mathrm{meas}}/[1 + n(\omega, T)]$.

improper ferroelectric phase transitions.[48] In Fig. 2(a), the IR and Raman activities of the low-frequency modes are shown around 100 K where the modes are better resolved. It is clear that α is both IR and Raman active, experimental evidence that the real space group is of lower symmetry than the centrosymmetric $Pbca$ structure resolved by x-ray diffraction; the temperature dependence of the mode positions is shown in Fig. 4(a) (triangles for IR and circles for Raman activity, respectively). We note that an IR active mode also is observed at 33 cm^{-1}, which can be ascribed to a shear mode as depicted in Table II. We cannot disregard the possibility of the β mode also being IR active; a weak IR mode is observed at the same frequency, but the assignment is not as reliable as for the α mode.

Similar modes have been observed previously but, in different studies, were assigned to either octahedral rotations[79] or organic librations.[80] To shed more light on the origin of these modes, we also measured the low energy $a'(cc)\overline{a'}$ spectra of $(C_6H_5CH_2CH_2NH_3)_2MnCl_4$ (PEAMnCl) and $(CH_3CH_2NH_3)_2CuCl_4$ (EACuCl) in which the first compound has the same organic constituent as PEACuCl but a different $3d$ element, and the second compound has the same inorganic constituent but a different smaller organic molecule [see Fig. 2(a)]. We note that EACuCl and PEACuCl have a similar buckling angle for the octahedra and the same magnitude of Jahn-Teller distortion. The low-energy modes of PEAMnCl are observed at frequencies similar to those of PEACuCl, but there are significant mismatches with respect to the modes of EACuCl. This strongly suggests that these modes are not associated with the buckling of the distorted CuCl octahedra but rather have an organic origin. Both group-theory analysis[16] and our DFT calculation suggest that the low-frequency modes are consistent with the shear modes described in Table II.

A possible description of the low-frequency modes is given by a group-theoretical analysis of the phase-transition sequence $I4/mmm \rightarrow Cmca \rightarrow Pbca$ ($D_{4h}^{17} \rightarrow D_{2h}^{18} \rightarrow D_{2h}^{15}$) described in Ref. 16. This phase cascade was explained in terms of the slowing down of the hindered rotation of the NH$_3$ group. The $Cmca \rightarrow Pbca$ transition, analogous to the
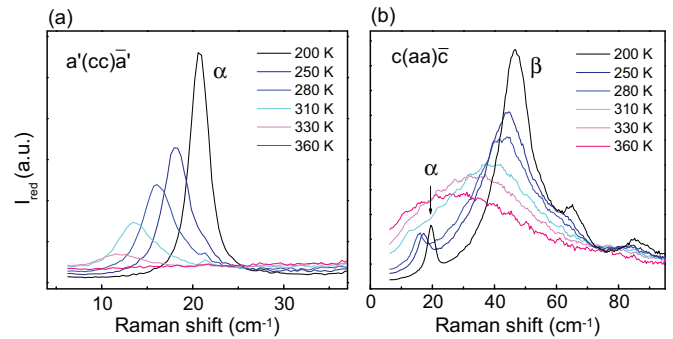
transition inferred from x-ray diffraction at 340 K in PEACuCl, happens at the Y point of the Brillouin zone, leading to unit-cell doubling and activation of a totally symmetric low-frequency mode in the Raman spectra. The soft-mode displacement pattern deduced from Ref. 16 can be represented as a shear mode of the organic layer with respect to the inorganic layer along the a' axis.[16,84] As shown below, the lowest-frequency mode α disappears at 340 K, an indication of coupling to the order parameter of the phase transition.

The shearlike character of the mode is further supported by the results of our DFT calculations where we find two low-frequency modes at ~25 cm^{-1}, which have a normal mode displacement consistent with the type-3 shear mode described in Table II. As mentioned above, the displacements correspond to a shear mode of the organic layer against the inorganic framework along one in-plane axis [see the inset of Fig. 2(b)]. Unfortunately, the low symmetry of the optimized structure found by the DFT calculations does not allow for an accurate analysis of the Raman/IR selection rules, which would allow the determination of an appropriate space group. It should be mentioned that the polar space group $P2_1$ is also compatible with the DFT-calculated structure but with larger acceptance. Another possibility is $P2_1ca$, which is obtained when a single glide plane is removed from the $Pbca$ structure. We currently have no preferential reason to choose either space group over $P1$, so the latter will be used from here on.

Figure 3 shows the low frequency $a'(cc)\overline{a'}$ and $c(aa)\overline{c}$ spectra at selected temperatures. These spectra are plotted in terms of the reduced intensity I_{red}, i.e., their measured intensities I_{meas} have been normalized by the population factor $1 + n(\omega, T)$, where $n(\omega, T)$ is the Bose-Einstein distribution function. At low temperatures, the α and β modes are found as narrow (resolution-limited) bands at 25 and 53 cm^{-1} (see Fig. 1; the room-temperature Raman shifts of these modes are 15 and 40 cm^{-1}, respectively). Apart from a small decrease in frequency and modest broadening, these modes essentially remain unchanged up to $T = 200$ K. Upon increasing the temperature further, both modes broaden and soften considerably. This continues up to $T_C = 340$ K, above which α disappears, whereas, β remains visible as a strongly
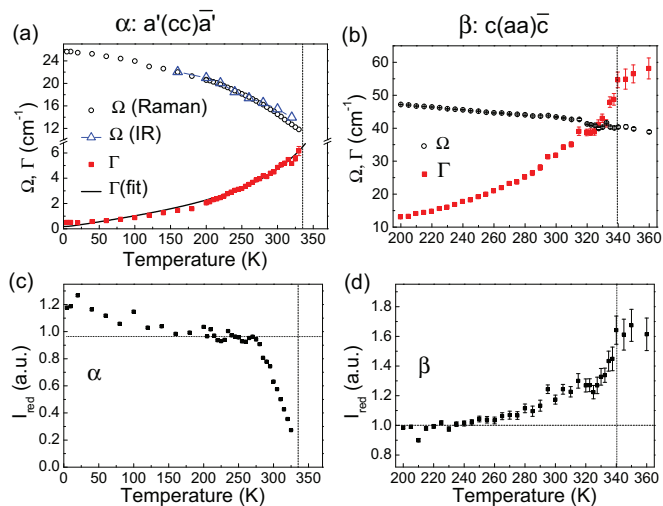
FIG. 4. (Color online) Raman shift Ω, width Γ, and strength I_{red} of the phonons (a) and (c) α and (b) and (d) β. The $a'(cc)\overline{a'}$ mode shows nonlinear softening and nonlinear linewidth broadening while heating (a). The strength I_{red} of (c) α is discontinuous and decreases to zero when approaching T_C from below. In contrast, the $c(aa)\overline{c}$ mode β does not disappear at T_C but is strongly overdamped.

overdamped broadband. To quantify these observations, we used a model consisting of a Debye relaxor mode in combination with Lorentz oscillators[83] to model the phonon bands,

$$I_{\mathrm{meas}}(\omega, T) = \frac{1}{\pi} \frac{\tau_{qe} I_{qe}}{\left(1 + \omega^2 \tau_{qe}^2\right)}$$
$$+ \sum_i \left(\frac{1}{\pi} \frac{I_i \Omega_i^2 \Gamma_i}{\left[\left(\omega^2 - \Omega_i^2\right)^2 + \Gamma_i^2 \omega^2\right]} [1 + n(\Omega_i, T)] \right).$$

Here, I_{qe} is the strength of the quasielastic (qe) scattering with relaxation time τ_{qe}, and I_i is the strength of the ith phonon response centered at Ω_i with width Γ_i (Γ_i represents the normal Lorentzian width when $\Omega_i \gg \Gamma_i$). All these parameters were left free during the fitting process. This equation describes the data very well. Figure 4 shows the resulting temperature dependence of the two low-energy modes α and β. Mode α [Figs. 4(a) and 4(b)] shows soft-mode behavior. Upon increasing temperature, the energy of this mode softens by more than 50%, and the linewidth broadens in nonlinear fashion. We note that the agreement between the IR and the Raman measurements of the mode position Ω_α is very good, which discounts the possibility of an accidental overlap of two different modes. The scattering strength of this mode shows particularly interesting behavior. Below 270 K, it is fairly constant, but it shows a steep decline upon further increasing the temperature until it disappears at the phase transition. Mode β [Figs. 4(c) and 4(d)] shows similar characteristics, exhibiting a nonlinear increase in its linewidth and a mode softening of its frequency upon approaching the phase transition from below. However, in the vicinity of the phase transition, the mode becomes overdamped, and it persists above the phase transition as a strongly overdamped mode. The mode intensity constantly

increases with temperature. For the α mode, the increase in linewidth is well described by the standard two-phonon decay process [$\Gamma \propto \{1 + 2/[\exp(\hbar\Omega_\alpha/2kT) + 1]\}$, see the fit in Fig. 4(a)]. The nonlinear increase in the width is due to mode position softening. Mode β shows a similar behavior, but a more accurate method of fitting and modeling the overdamped modes is required to interpret these results and is beyond the scope of this paper. However, it should be mentioned that the normal two-photon decay mechanism does not describe the data well, and models, such as the Andrade and Porto and Andrade *et al.* disorder models seem to be necessary.[85,86]

The behavior of the low-energy modes suggests that the phase transition has displacive character, probably in combination with the established order-disorder phenomena. The actual phase transition has a weak first-order nature, which is in line with the observation of temperature hysteresis in the heat capacity[40] and birefringence experiments. As will be discussed in the remainder of this paper, the low-energy mode α is coupled directly to the order parameter of this $T = 340$-K transition and is coupled indirectly to the polar nature of the room-temperature phase of PEACuCl.

V. DISCUSSION

As discussed above, the ferroelectric phase transition at 340 K in PEACuCl has a displacive nature in conjunction with order-disorder phenomena. Examples of the coexistence of order-disorder and displacive effects are known in the literature.[87,88] Pure displacive and pure order-disorder transitions can be understood as two limiting cases of a simple system:[89,90] a chain of atoms, elastically coupled, where each atom resides in a double-well potential. The transition is of order-disorder type when the elastic force is weak compared to the depth of the double well and is purely displacive in the opposite case. The order-disorder character of the high-temperature phase transition in layered organic-inorganic hybrids is well documented,[91] for instance, by Raman spectroscopy,[32] NMR,[24,26,91] and NQR (Ref. 23) studies and is interpreted in terms of a hopping probability of the NH_3 group between various minima in the multiwell potential generated by the distorted CuCl octahedra.[24] The soft-mode energy in pure order-disorder transitions does not go to zero at T_C, and an increase in the mode strength on approaching T_C and strong overdamping generally is observed. In contrast, the α mode remains well resolved even close to T_C. The fact that Ω_α does not soften down to zero at T_C might indicate a crossover from displacive to order-disorder. The organic-inorganic shear character of mode α demonstrates that, when investigating the physical properties of similar hybrids, the interplay and coupling between the organic and the inorganic constituents should be taken into account.

The intensity of mode α is coupled to the order parameter η of the transition. As discussed in Ref. 50, in the ordered phase, the totally symmetric soft mode is always R active, but it is also IR active only if the ordered phase belongs to a polar class. The Raman selection rules for the α mode (see Table III) suggest that α is totally symmetric; α would have A_g symmetry in $Pbca$. The THz experiments prove the IR activity of the
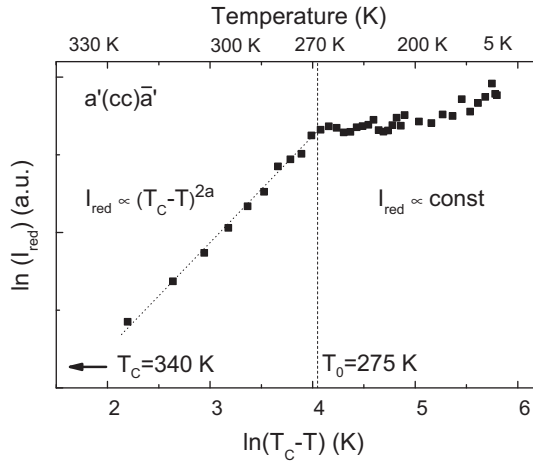
FIG. 5. Bilogarithmic plot of the strength I_{red} of the lowest-energy phonon α as a function of $(T_C - T)$. Below $(T_C - \Delta T)$, the system is stable, and the mode strength is constant. A continuous symmetry modification sets in between $T_C - \Delta T$ and T_C, and the strength decreases as $I_{red} \propto (T_C - T)^{2a}$. Since the phonon amplitude is coupled directly to the order parameter η of the ferroelectric phase transition,[40,48] I_{red} describes the appearance of polar order below T_C.

mode, suggesting that the phase of PEACuCl below T_C is, indeed, polar. The strength decrease in α is consistent with the soft-mode behavior of improper ferroelectrics.[48] Assuming the lowest-order interaction of the polarization P with the order parameter (the term $P\eta^2$ in the free-energy expansion, but the term depends on the crystal structure[50]), the phonon strength is proportional to the square of the order parameter η,

$$I_{T<T_C} = \gamma \eta^2, \qquad (1)$$

where γ represents the coupling between the order parameter and the mode strength. The order parameter η can be expressed by a critical exponent a,[50] defined by

$$\eta \propto (T_C - T)^a. \qquad (2)$$

Figure 5 shows a bilogarithmic plot of the temperature dependence of the strength of mode α. Between phase transition and 270 K, this mode strength shows the expected power-law behavior $I \propto (T_C - T)^{2a}$ with critical exponent $a = 0.33 \pm 0.08$ in very good agreement with the exponents observed for similar phase transitions.[18,91,92] We note that the critical behavior holds over a very broad temperature range of ΔT: $\Delta T \simeq 0.2 \times T_C$ as observed in various cases.[93]

Finally, we turn to the polar nature of the room-temperature phase of PEACuCl. The ferroelectric polarization as well as mode α as just discussed, are coupled to the order parameter of the phase transition.[40] The displacements of the eigenvector of mode α represent, at least, qualitatively, the distortion happening at $T_C = 340$ K. In agreement with the phase-transition sequence $Cmca \rightarrow Pbca$ ($D_{2h}^{18} \rightarrow D_{2h}^{15}$, high-to-low-temperature phase) as studied in Ref. 16, the phase-transition soft mode is a linear combination of octahedral and cationic librations (note that the buckling of the octahedra also contributes to the displacement pattern of the soft mode

in agreement with Ref. 40), represented as type-3 shear of Table II. Such a mode also is, indeed, obtained by our DFT calculations at a frequency of ~ 25 cm^{-1} in good agreement with the observed Raman/IR shift in α ($\Omega_\alpha \sim 25$ cm^{-1} at 4 K). The condensation of such a mode would lead to a tilt of the organic molecules with respect to the inorganic framework. Since the electric dipole of the PEA cations is 13 D (1 D = 3.34×10^{30} C m),[94] this, indeed, leads to a polar state, provided that the tilt angle alternates in the direction perpendicular to the layered structure, which is the case for the type-3 mode. A tilt angle of the cations with respect to the c axis [according to the type-3 mode in Table II and Fig. 2(b)] of only $\sim 0.07°$ is sufficient to explain the observed polarization density of 250 μC/m^2.[40] Such a tilt angle would be difficult or impossible to observe using standard x-ray-diffraction techniques.[58] Although this tilting of the organic molecule in PEACuCl may fully explain the observed magnitude of the polarization, it is expected that hydrogen-bond ordering of the ammonium ion as discussed in Ref. 40 may also play a role. Assuming the tilt to be the main mechanism of the ferroelectricity, the observed polarization should increase proportionally to the intrinsic dipole moment of the organic molecule.

VI. CONCLUSION

The data presented here clearly demonstrate the displacive aspects of the 340-K ferroelectric phase transition in PEACuCl. The continuous structural modification, probed by the intensity of a low-frequency Raman/IR mode (α in the text), sets in at ~ 270 K and is concluded at $T_C = 340$ K with a first-order-like transition (already demonstrated in Ref. 40). We suggest that the polar order of the room-temperature phase of PEACuCl arises from a tilt of the organic molecules with respect to the inorganic plane that alternates in the c direction (see the type-3 mode, Table II). The predicted tilt of the organic cations of $\sim 0.07°$ might be beyond the sensitivity of x-ray-diffraction measurements. Contrary to the existing literature where only the orientational dynamics of the organic cation have been discussed, we have shown that the physical properties of this family of hybrids are determined by the interplay between the inorganic and the organic constituents.

Most of the CuCl$_4$-based compounds[19,21,22] undergo a similar phase transition in the range between 320 and 360 K. In analogy to the present example of PEACuCl, the apparent $Cmca \rightarrow Pcba$ ($D_{2h}^{18} \rightarrow D_{2h}^{15}$) (Ref. 50) transitions reported in other CuCl$_4$-type hybrids might actually be ferroelectric transitions to symmetries lower than $Pbca$.

*pvl@ph2.uni-koeln.de

[1] C. N. R. Rao, A. K. Cheetham, and A. Thirumurugan, J. Phys.: Condens. Matter **20**, 083202 (2008).

[2] S. R. Batten, N. R. Champness, X.-M. Chen, J. Garcia-Martinez, S. Kitagawa, L. Öhrström, M. O'Keeffe, M. P. Suh, and J. Reedijk, CrystEngComm **14**, 3001 (2012).

[3] H. K. Chae, D. Y. Siberio-Pérez, J. Kim, Y. Go, M. Eddaoudi, A. J. Matzger, M. O'Keeffe, and O. M. Yaghi, Nature (London) **427**, 524 (2004).

[4] U. Mueller, M. Schubert, F. Teich, H. Puetter, K. Schierle-Arndt, and J. Pastré, J. Mater. Chem. **16**, 626 (2006).

[5] D. Mitzi, J. Chem. Soc., Dalton Trans. 2001, 1 (2000).

[6] L. J. de Jongh and A. R. Miedema, Adv. Phys. **23**, 1 (1974).

[7] K. S. Aleksandrov and J. Bartolome, Phase Trans. **74**, 255 (2001).

[8] D. B. Mitzi, Prog. Inorg. Chem. **48**, 1 (1999).

[9] R. Dingle, M. E. Lines, and S. L. Holt, Phys. Rev. **187**, 643 (1969).

[10] B. Gerstein, F. Gehring, and R. Willett, J. Appl. Phys. **43**, 1932 (1972).

[11] W. D. van Amstel and L. J. de Jongh, Solid State Commun. **11**, 1423 (1972).

[12] J. Koppen, R. Hamersma, J. V. Lebesque, and A. R. Miedema, Phys. Lett. A **25**, 376 (1967).

[13] N. D. Mermin and H. Wagner, Phys. Rev. Lett. **17**, 1133 (1966).

[14] L. J. de Jongh, W. D. van Amstel, and A. R. Miedema, Physica **15**, 277 (1972).

[15] W. E. Estes, D. B. Losee, and W. E. Hatfield, J. Chem. Phys. **72**, 630 (1980).

[16] J. Petzelt, J. Phys. Chem. Solids **36**, 1005 (1975).

[17] H. Arend, R. Hofmann, and F. Waldner, Solid State Commun. **13**, 1629 (1973).

[18] K. Knorr, I. R. Jahn, and G. Heger, Solid State Commun. **15**, 231 (1974).

[19] I. R. Jahn, K. Knorr, and J. Ihringer, J. Phys.: Condens. Matter **1**, 6005 (1989).

[20] M. J. Tello, J. L. Manes, J. Fernandez, M. A. Arriandiaga, and J. M. Perez-Mato, J. Phys. C **14**, 805 (1981).

[21] G. Heygster and W. Kleemann, Physica B & C **89**, 165 (1977).

[22] W. Kleemann and F. J. Schafer, Physica B & C **97**, 145 (1979).

[23] R. Kind and J. Roos, Phys. Rev. B **13**, 45 (1976).

[24] R. Kind, S. Pleško, H. Arend, R. Blinc, B. Žekš, J. Seliger, B. Ložar, J. Slak, A. Levstik, C. Filipič, V. Žagar, G. Lahajnar, F. Milia, and G. Chapuis, J. Chem. Phys. **71**, 2118 (1979).

[25] M. Kozelj, V. Rutar, I. Zupancic, and R. Blinc, J. Chem. Phys. **74**, 4123 (1981).

[26] P. Muralt, R. Kind, and W. Buhrer, Phys. Rev. B **38**, 666 (1988).

[27] W. Kleemann, F. Schfer, E. Krjmki, R. Laiho, and T. Levola, Physica B & C **119**, 269 (1983).

[28] R. Geick and K. Strobel, J. Phys. C **12**, 27 (1979).

[29] L. Ricard and J. C. Lassegues, J. Phys. C **17**, 217 (1984).

[30] T. Goto, B. Lüthi, R. Geick, and K. Strobel, Phys. Rev. B **22**, 3452 (1980).

[31] T. Goto, M. Yoshizawa, A. Tamaki, and T. Fujimura, J. Phys. C **15**, 3041 (1982).

[32] M. Couzi, A. Daoud, and R. Perret, Phys. Status Solidi A **41**, 271 (1977).

[33] Z. Iqbal, H. Arend, and P. Wachter, J. Phys. C **13**, 4757 (1980).

[34] R. Mokhlisse, M. Couzi, and P. L. Loyzance, J. Phys. C **16**, 1367 (1983).

[35] I. Pabst, J. Karoly, H. Fuess, and M. Couzi, Phys. Status Solidi A **155**, 341 (1996).

[36] R. Mokhlisse, N. B. Chanh, M. Couzi, Y. Haget, and C. Hauw, J. Phys. C **17**, 233 (1984).

[37] R. Geick and K. Strobel, J. Phys. C **10**, 4221 (1977).

[38] F. J. Zuniga, M. J. Tello, J. M. P. Mato, M. A. P. Jubindo, and G. Chapuis, J. Chem. Phys. **76**, 2610 (1982).

[39] H. Hagemann and H. Bill, J. Phys. C **18**, 6441 (1985).

[40] A. O. Polyakov, A. H. Arkenbout, J. Baas, G. R. Blake, A. Meetsma, A. Caretta, P. H. M. van Loosdrecht, and T. T. M. Palstra, Chem. Mater. **244**, 133 (2012).

[41] B. Kundys, A. Lappas, M. Viret, V. Kapustianyk, V. Rudyk, S. Semak, C. Simon, and I. Bakaimi, Phys. Rev. B **81**, 224434 (2010).

[42] E. Fantuzzo and R. Nitsche, Phys. Rev. **117**, 936 (1960).

[43] P. S. Peercy, B. Morosin, and G. A. Samara, Phys. Rev. B **8**, 3378 (1973).

[44] P. S. Ghalsasi and K. Inoue, Polyhedron **28**, 1864 (2009).

[45] P. Jain, V. Ramachandran, R. J. Clark, H. D. Zhou, B. H. Toby, N. S. Dalal, H. W. Kroto, and A. K. Cheetham, J. Am. Chem. Soc. **131**, 13625 (2009).

[46] R. Ramesh, Nature (London) **461**, 1218 (2009).

[47] W. Cochran, Adv. Phys. **9**, 387 (1960).

[48] V. Dvořák and J. Petzelt, Phys. Lett. A **35**, 209 (1971).

[49] T. Shigenari, Phys. Lett. A **46**, 243 (1973).

[50] J. Petzelt, Phys. Lett. A **48**, 341 (1974).

[51] R. H. Lyddane, R. G. Sachs, and E. Teller, Phys. Rev. **59**, 673 (1941).

[52] Y. Ishibashi and Y. Takagi, Jpn. J. Appl. Phys. **15**, 1621 (1976).

[53] J. F. Scott, Rev. Mod. Phys. **46**, 83 (1974).

[54] J. Petzelt and V. Dvorak, J. Phys. C **9**, 1571 (1976).

[55] H. Arend and W. Huber, J. Cryst. Growth **43**, 213 (1978).

[56] R. D. Willett, J. A. Haugen, J. Lebsback, and J. Morrey, Inorg. Chem. **13**, 2510 (1974).

[57] V. B. Kapustianik, Phys. Status Solidi B **204**, 877 (1997).

[58] R. D. Willett, Acta Crystallogr. Sect. C: Cryst. Struct. Commun. **46**, 565 (1990).

[59] A. H. Arkenbout, T. Uemura, J. Takeya, and T. T. M. Palstra, Appl. Phys. Lett. **95**, 173104 (2009).

[60] A. H. Arkenbout, Ph.D. thesis, University of Groningen, 2010.

[61] G. Burns, Phys. Rev. B **13**, 215 (1976).

[62] M. Cohen and T. L. Einstein, Phys. Rev. B **7**, 1932 (1973).

[63] T. T. A. Lummen, I. P. Handayani, M. C. Donker, D. Fausti, G. Dhalenne, P. Berthet, A. Revcolevschi, and P. H. M. van Loosdrecht, Phys. Rev. B **77**, 214310 (2008).

[64] P. Zolfaghari, G. A. de Wijs, and R. A. de Groot, J. Phys.: Condens. Matter **25**, 295502 (2013).

[65] R. Dovesi, R. Orlando, B. Civalleri, C. Roetti, V. R. Saunders, and C. M. Zicovich-Wilson, Z. Kristallogr.-Cryst. Mater. **220**, 571 (2005).

[66] R. Dovesi, V. R. Saunders, C. Roetti, R. Orlando, C. M. Zicovich-Wilson, F. Pascale, B. Civalleri, K. Doll, N. M. Harrison, I. J. Bush, P. D'Arco, and M. Llunell, CRYSTAL09 *User's Manual* (University of Torino, Torino, 2009).

[67] F. Pascale, C. M. Zicovich-Wilson, F. López Gejo, B. Civalleri, R. Orlando, and R. Dovesi, J. Comput. Chem. **25**, 888 (2004).

[68] C. M. Zicovich-Wilson, F. Pascale, C. Roetti, V. R. Saunders, R. Orlando, and R. Dovesi, J. Comput. Chem. **25**, 1873 (2004).

[69] K. Doll and N. Harrison, Chem. Phys. Lett. **317**, 282 (2000).

[70]E. Apra, M. Causa, M. Prencipe, R. Dovesi, and V. R. Saunders, J. Phys.: Condens. Matter **5**, 2969 (1993).

[71]M. Catti, A. Pavese, R. Dovesi, and V. R. Saunders, Phys. Rev. B **47**, 9189 (1993).

[72]J. S. Binkley, J. A. Pople, and W. J. Hehre, J. Am. Chem. Soc. **102**, 939 (1980).

[73]P. C. Harihara and J. Pople, Theor. Chim. Acta **28**, 213 (1973).

[74]http://www.crystal.unito.it/Basis_Sets/Ptable.html

[75]H. J. Monkhorst and J. D. Pack, Phys. Rev. B **13**, 5188 (1976).

[76]A. Lucken, H. Hagemann, and H. Bill, J. Phys.: Condens. Matter **3**, 5085 (1991).

[77]F. Zouari and A. B. Salah, Solid State Sci. **6**, 847 (2004).

[78]Y. Abid, M. Kamoun, A. Daoud, and F. Romain, J. Raman Spectrosc. **21**, 709 (1990).

[79]Z. Iqbal, H. Arend, and P. Wachter, J. Phys. C **14**, 1497 (1981).

[80]R. Mokhlisse, M. Couzi, N. B. Chanh, Y. Haget, C. Hauw, and A. Meresse, J. Phys. Chem. Solids **46**, 187 (1985).

[81]R. Mokhlisse, M. Couzy, and J. C. Lassegues, J. Phys. Chem. Solids **16**, 1353 (1983).

[82]T. Schneider, G. Srinivasan, and C. P. Enz, Phys. Rev. A **5**, 1528 (1972).

[83]M. E. Lines and A. M. Glass, *Principles and Applications of Ferroelectrics and Related Materials* (Clarendon, Oxford, 1977).

[84]O. V. Kovalev, *Irreducible Representations of the Space Groups* (Gordon and Breach, New York, 1965).

[85]P. da R. Andrade and S. P. S. Porto, Solid State Commun. **13**, 1249 (1973).

[86]P. da R. Andrade, A. D. Prasad Rao, R. S. Katiyar, and S. P. S. Porto, Solid State Commun. **12**, 847 (1973).

[87]N. Dalal, A. Klymachyov, and A. Bussmann-Holder, Phys. Rev. Lett. **81**, 5924 (1998).

[88]E. Buixaderas, S. Kamba, and J. Petzelt, Ferroelectrics **308**, 131 (2004).

[89]S. Aubry, J. Chem. Phys. **62**, 3217 (1975).

[90]M. T. Dove, Am. Mineral. **82**, 213 (1997).

[91]R. Kind, S. Plesko, P. Gunter, J. Roos, and J. Fousek, Phys. Rev. B **23**, 5301 (1981).

[92]P. Prasad and H. Bist, J. Phys. Chem. Solids **50**, 1033 (1989).

[93]W. Dultz, J. Chem. Phys. **65**, 2812 (1976).

[94]Estimations of the dipole moments of C_6H_5-CH_2CH_2-NH_3^+ (PEA^+) and CH_3-CH_2-NH_3^+ (EA^+) were obtained by a DFT PBE/6-311G** calculation (GAMESS-UK,[95] geometries were optimized at PBE/6-311G**) and were found to be 13 and 4 D, respectively.

[95]M. F. Guest, I. J. Bush, H. J. J. van Dam, P. Sherwood, J. M. H. Thomas, J. H. van Lenthe, R. W. A. Havenith, and J. Kendrick, Mol. Phys. **103**, 719 (2005).